pH-Dependent Equilibrium Isotope Fractionation Associated with the Compound Specific Nitrogen and Carbon Isotope Analysis of Substituted Anilines by SPME-GC/IRMS

ARTICLE *in* ANALYTICAL CHEMISTRY · FEBRUARY 2011

Impact Factor: 5.64 · DOI: 10.1021/ac102667y · Source: PubMed

6 AUTHORS, INCLUDING:

Marita Skarpeli-Liati
Eawag: Das Wasserforschungs-Institut des E…
8 PUBLICATIONS **119** CITATIONS
SEE PROFILE

William A Arnold
University of Minnesota Twin Cities
119 PUBLICATIONS **3,912** CITATIONS
SEE PROFILE

Christopher J Cramer
University of Minnesota Twin Cities
532 PUBLICATIONS **23,506** CITATIONS
SEE PROFILE

analytical chemistry

ARTICLE

pubs.acs.org/ac

pH-Dependent Equilibrium Isotope Fractionation Associated with the Compound Specific Nitrogen and Carbon Isotope Analysis of Substituted Anilines by SPME-GC/IRMS

Marita Skarpeli-Liati,[†] Aurora Turgeon,[§] Ashley N. Garr,[§] William A. Arnold,[‡] Christopher J. Cramer,[§] and Thomas B. Hofstetter[†,*]

[†] Eawag, Swiss Federal Institute of Aquatic Science and Technology, CH-8600 Dübendorf and Institute of Biogeochemistry and Pollutant Dynamics (IBP), ETH Zurich, CH-8092 Zurich, Switzerland,

[‡]Department of Civil Engineering, University of Minnesota, [§]Department of Chemistry and Supercomputing Institute, University of Minnesota, Minneapolis, Minnesota 55455, United States

Supporting Information

ABSTRACT: Solid-phase microextraction (SPME) coupled to gas chromatography/isotope ratio mass spectrometry (GC/IRMS) was used to elucidate the effects of N-atom protonation on the analysis of N and C isotope signatures of selected aromatic amines. Precise and accurate isotope ratios were measured using polydimethylsiloxane/divinylbenzene (PDMS/DVB) as the SPME fiber material at solution pH-values that exceeded the pK_a of the substituted aniline's conjugate acid by two pH-units. Deviations of $\delta^{15}N$ and $\delta^{13}C$-values from reference measurements by elemental analyzer IRMS were small (<0.9‰) and within the typical uncertainties of isotope ratio measurements by SPME-GC/IRMS. Under these conditions, the detection limits for accurate isotope ratio measurements were between 0.64 and 2.1 mg L^{-1} for $\delta^{15}N$ and between 0.13 and 0.54 mg L^{-1} for $\delta^{13}C$, respectively. Substantial inverse N isotope fractionation was observed by SPME-GC/IRMS as the fraction of protonated species increased with decreasing pH leading to deviations of −20‰ while the corresponding $\delta^{13}C$-values were largely invariant. From isotope ratio analysis at different solution pHs and theoretical calculations by density functional theory, we derived equilibrium isotope effects, EIEs, pertinent to aromatic amine protonation of 0.980 and 1.001 for N and C, respectively, which were very similar for all compounds investigated. Our work shows that N-atom protonation can compromise accurate compound-specific N isotope analysis of aromatic amines.

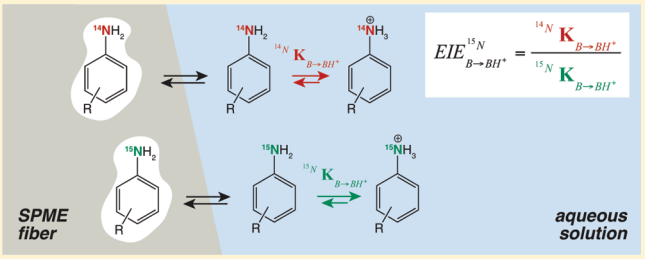

INTRODUCTION

Assessing transformation processes of organic micropollutants is crucial for addressing the risks of soil and water contamination. Compound-specific isotope analysis (CSIA) offers a complementary approach for identifying contaminant sources and degradation pathways, as well as for quantifying the extent of a transformation reaction even if several processes take place simultaneously. Because CSIA reveals the reactive position within an organic compound via detection of changes in isotopic composition, stable isotope ratio measurements also provide crucial information about the underlying reaction mechanism.[1] While CSIA is widely applied for the investigation of groundwater contaminants such as chlorinated solvents (polychlorinated alkenes[2−5]) and fuel components (methyl-tert butyl ether,[6−8] benzene,[9] toluene[10−12]), combined multielement isotope-fractionation analysis involving the elements C, H, and N is emerging for the transformation assessment of agrochemicals, explosives, and other priority pollutants.[13−15] In fact, micropollutants exhibiting N-containing functional groups are the most promising target molecules for CSIA, because the presence of N functional groups is key for many transformation processes including reductions, oxidations, substitutions, and eliminations.[16] Despite the importance of these reaction pathways, only few N-containing organic micropollutants are amenable to CSIA.

To date, nitrogen isotope fractionation has been successfully measured by GC/IRMS of amino acids,[17−19] selected N-containing herbicides,[13,20,21] and nitroaromatic compounds.[11,14,22,23] To expand the applicability of CSIA, this study targets the N isotope analysis of substituted aromatic amines by GC/IRMS. Substituted anilines represent a class of toxic and mutagenic environmental pollutants[24] and they have also served as model compounds for studying the transformation of emerging contaminants such as sulfonamide antibiotics.[25] In contaminated environments, abiotic as well as microbial oxidation and addition reactions occur either directly at the nitrogen atom of the primary amino group[26−28] or via oxidation at the aromatic ring.[29] The availability of analytical methods for the precise and accurate measurement of N and C isotope ratios is therefore essential for

Received: October 8, 2010
Accepted: January 4, 2011
Published: February 08, 2011

assessing degradation pathways of substituted anilines in the environment.

Current approaches to isotope ratio measurements of substituted anilines in aqueous solutions by GC/IRMS coupled to solid phase microextraction (SPME), however, showed poor accuracy, that is, deviations from the correct N isotope signatures were above 2‰.[14] Moreover, the consequences of aromatic amine protonation on the sensitivity and accuracy of CSIA is unexplored. Protonation of the anilines at pH values <7 deteriorates extraction efficiencies of the analytes from the aqueous solution to the SPME-fiber, because only neutral species can be expected to adsorb to the nonpolar fiber coating and thus be measured by CSIA. Given that environmentally relevant pH-ranges coincide with the pK_a-values of many protonated aromatic amines (typical pK_a between 2.5 and 7,[16,30]) and that N atom protonation might be key for understanding the isotope fractionation of N-containing micropollutants,[31,32] the impact of equilibrium isotope fractionation on the isotope ratio analysis of aromatic amines requires closer examination.

It was the goal of this study to investigate how aromatic amino group protonation affects the sensitivity and accuracy of N and C isotope signatures, δ^{15}N and δ^{13}C, of substituted primary aromatic amines while measured by SPME-GC/IRMS and whether significant N and C equilibrium isotope effects (EIE) are associated with proton exchange reactions. To this end, we examined the accuracy and precision of δ^{15}N and δ^{13}C-values of a series of substituted anilines in aqueous samples in the pH-range 2.0−7.0 in the presence of various buffers. The compounds were chosen so that their pK_a-values (2.5−5.1) enabled us to study the effect of protonation on SPME-GC/IRMS under the chosen experimental conditions. Equilibrium isotope effects associated with aromatic amine protonation were determined experimentally and compared to independent estimates obtained from density functional theory calculations.

EXPERIMENTAL SECTION

Safety Considerations. Substituted anilines are toxic and potentially carcinogenic. When dealing with anilines, wear suitable clothing, gloves, and work in a well-ventilated fume hood.

Reagents and Materials. All chemicals in this study were used as received. The substituted anilines examined included aniline (≥99.5%, Fluka), 2-methylaniline (≥99.5%, Merck), 4-methylaniline (≥99%, Merck), 2-chloroaniline (≥99.5%, Aldrich), and 4-chloroaniline (≥99%, Fluka). Buffers used were sodium acetate trihydrate ($NaC_2H_3O_2 \cdot 3H_2O$, puriss, Riedel-de Haën), potassium phosphate dibasic (K_2HPO_4, puriss, Riedel-de Haën), sodium citrate tribasic dihydrate ($Na_3C_6H_5O_7 \cdot 2H_2O$, ≥99%, Fluka) and 2-morpholinoethanesulfonic acid monohydrate (MES, $C_6H_{13}NO_4S \cdot H_2O$, ≥99%, Fluka). All buffer solutions were prepared in deionized water (18.2 MΩ·cm, NANOpure) and solution pH-values were adjusted with hydrochloric acid (Sigma Aldrich) and sodium hydroxide solution (Fluka). Solvents used were methanol (>99.9%, Scharlau, Spain) and ethyl acetate (>99.8%, Riedel-de Haën). High purity Ar was used for deoxygenation of water and methanol and helium, nitrogen, and carbon dioxide were used for GC/MS and GC/IRMS measurements (all ≥99.999%, Carbagas).

Instrumentation. Prior to nitrogen and carbon isotope analysis, extraction efficiencies of the substituted anilines from the buffered aqueous solutions to the SPME-fibers were evaluated by means of GC/MS analysis. Instrumentation and procedures for chromatographic separation used for GC/MS analysis were similar to that of previous studies.[14] A GC (Trace GC Ultra, Thermo Electron Corp.) was combined with a quadrupole MS (Trace DSQ ESI 250, Thermo Electron Corp.) and a CombiPAL autosampler (CTC) and equipped with a cold on-column and a split/splitless injector with a Merlin Microseal (Merlin Instrument Co.). The isotope analysis was carried out using a Trace GC (Thermo Electron Corp.) coupled to an isotope ratio mass spectrometer (IRMS; Delta V PLUS, Thermo Electron Corp.) via a combustion interface (GC Combustion III).[33] Helium carrier gas was used at constant pressure of 100 kPa. For chromatographic separation, 1 m of a deactivated guard column (530 μm i.d., BGB, Boeckten, Switzerland) and a 30 m × 0.32 mm fused-silica column (Zebron, ZB-5-ms, 0.25 μm, Phenomenex) were used. The applied temperature program was 1 min at 50 °C, followed by a 10 °C/min ramp to 250 °C and 5 min at 250 °C.

For the δ^{13}C measurements the NiO/CuO/Pt wires of the combustion unit were oxidized with O_2 during 12 h prior to use at 940 °C. The N isotope signatures were measured with the same oxidation reactor but without preoxidation at 980 °C. The temperature of the reduction reactor was 650 °C. Additionally, liquid nitrogen was used to trap the CO_2 produced during combustion of the analytes to prevent isobaric interferences by CO^+-fragments.[34]

SPME of Aqueous Samples. The SPME fiber coating polyacrylate (PA, 85 μm, Supelco), used for the nitroaromatic compounds,[14] was compared to polydimethylsiloxane/divinylbenzene (PDMS/DVB, 65 μm, Supelco). Both materials led to reproducible measurements and enabled more than 100 injections per fiber according to the following procedure. 1.3 mL of buffered solution was transferred into 2 mL autosampler glass vials, which contained 0.30 g of NaCl (final ionic strength I of 4 M). The samples were shaken on a Vortex shaker to dissolve NaCl. The SPME fiber was immersed directly into the buffered aqueous solutions and the analytes were allowed to adsorb on the fiber for 45 min at 40 °C. Thermal desorption from the SPME-fiber was performed in a split/splitless injector equipped with a deactivated liner at 270 °C for 3 min. All measurements were carried out in triplicates. The SPME fiber was conditioned for 30 min at 250 °C after 20 samples.

Extraction Efficiency. To determine the efficiency of substituted aniline extraction from buffered aqueous solutions by the SPME fibers, calibration curves of the analytes were measured on the GC/MS after cold on-column injection and compared to peak areas obtained after solid-phase microextraction. The ratio of the slopes of the calibration curves for SPME- vs on-column-GC/MS (i.e., peak areas per amount of analyte in water vs ethyl acetate) was used as measure for the extraction efficiency of each compound (Table 1). Additionally, the preconcentration factors for both SPME-fibers were determined as ratios of the analyte concentrations in water or ethyl acetate, which are necessary for the detection of identical peak areas by SPME- vs on-column-GC/MS. Analyte solutions for cold on-column measurements (25 °C, 1 μL injection volume) were prepared in ethyl acetate and covered a concentration range of 5−50 μM. The SPME measurements were prepared in 10 mM MES buffer at pH 7 and the concentrations were typically between 1 and 10 μM to obtain peak areas similar to those measured by the cold on-column injection. Extraction efficiencies with the PDMS/DVB coated fiber were higher than with PA by a factor of 2 (4-Cl-aniline) to 13 (aniline, Table 1) for all substituted anilines used in this study. If not mentioned explicitly, the presented δ^{15}N and δ^{13}C values are measured with the PDMS/DVB-coated fiber.

Table 1. Names and Abbreviations of the Investigated Substituted Anilines as well as pK_a-Values of the Conjugate Acids. Extraction Efficiencies and Preconcentration Factors Obtained by SPME-GC/MS are Listed for Polyacrylate (PA) and Polydimethylsiloxane/Divinylbenzene (PDMS/DVB) as the Fiber Material[a]

compound name (abbreviation)	pK_a[16,58]	extraction efficiency[b] PA-fiber (%)	preconcentration factor PA-fiber (−)	extraction efficiency PDMS/DVB-fiber (%)	preconcentration factor PDMS/DVB-fiber (−)
aniline (An)	4.63	0.96 ± 0.03	12.5 ± 0.4	12.7 ± 0.4	165 ± 5
2-methyl-aniline (2-CH_3-An)	4.45	3.51 ± 0.10	45.6 ± 1.3	-	-
4-methyl-aniline (4-CH_3-An)	5.10	5.10 ± 0.20	66.3 ± 2.7	38.3 ± 1.1	497 ± 15
2-chloro-aniline (2-Cl-An)	2.46	9.73 ± 0.22	127 ± 3	-	-
4-chloro-aniline (4-Cl-An)	3.98	9.56 ± 0.38	124 ± 5	19.2 ± 1.1	250 ± 14

[a] All extraction experiments were performed after addition of NaCl to 10 mM MES buffer solution at pH 7.0 (I = 4 M). [b] See text for definition of extraction efficiencies and preconcentration factors.

Stable Isotope Measurements in buffered solutions with SPME-GC/IRMS. ^{15}N and ^{13}C signatures of the substituted anilines were measured after SPME and compared to isotope ratio measurements after on-column injection and to reference isotope ratios determined by elemental analyzer (EA, Carlo Erba) coupled to IRMS (Fisons Optima).[35] These comparisons were performed to evaluate whether isotopic fractionation occurred during SPME and/or combustion to analyte gases. Isotope signatures were measured as single compounds by SPME-GC/IRMS to avoid potential interferences from competitive adsorption of the analytes on the SPME fiber. The concentration range of the investigated anilines varied from 25 to 500 μM and 1−30 μM at pH 7 for $\delta^{15}N$ and $\delta^{13}C$, respectively, depending on the SPME extraction efficiency of each compound. The sensitivity of the $\delta^{15}N$-SPME analysis was 1.5 orders of magnitude lower compared to $\delta^{13}C$-SPME analysis as noted previously.[14] All $\delta^{15}N$- and $\delta^{13}C$-values are reported relative to air ($\delta^{15}N_{air}$) and Vienna PeeDee Belemnite ($\delta^{13}C_{VPDB}$), respectively, in per mil (‰).

$$\delta^h E = (R_{sample}/R_{standard} - 1) \times 1000 \quad (1)$$

where δ^hE is the element's isotope signature, R_{sample} and $R_{standard}$ are the isotope ratio of sample and standard, respectively. To exclude nonlinearity effects, which may arise due to variations of the introduced mass into the IRMS and lead to inaccurate isotope signatures,[36] we determined the concentration range within which isotope signatures, both $\delta^{15}N$ and $\delta^{13}C$, did not show any mass bias. The accuracy of the isotope measurements, $\Delta\delta^hE$, was expressed as deviation of the isotope signature measured by SPME-GC/IRMS, $\delta^hE_{SPME\text{-}GC/IRMS}$, from the reference isotope signature determined by EA-IRMS,[37] δ^hE_{ref} (eq 2).

$$\Delta\delta^h E = \delta^h E_{SPME\text{-}GC/IRMS} - \delta^h E_{ref} \quad (2)$$

Isotope fractionation during the adsorption of aromatic amines to SPME fibers was ruled out from measurements of $\delta^{15}N$ and $\delta^{13}C$-values measured with two different fiber materials (PA and PDMS/DVB) and comparison to isotope signatures determined after cold on-column injection of the analytes into the GC/IRMS system. No significant difference in accuracy between the two fiber coating materials was observed under optimized conditions (see discussion below), except for 4-Cl-aniline where extraction with the PDMS/DVB fiber decreased the $\Delta\delta^{15}N$ value by approximately 4‰.

pH-dependent isotope fractionation was investigated by SPME-GC/IRMS at several pH-values using 10 mM solutions of the following buffers (parentheses indicate pK_a-values) at ionic strength of 4 M (NaCl): MES (6.15) was used for the pH-range 5.0−7.0, acetate (4.76) for the pH 4.0−5.0, citrate (3.13 and 4.76) for pH 3.0−5.5, succinate (4.21 and 5.64) for pH 3.5−6.5, and phosphate (2.15) for pH 2.0. To avoid potential artifacts from acid-catalyzed modification of SPME-fibers, experiments were not run at pH-values below 2.0 thus limiting the extent to which the effect of protonation on N and C isotope analyses could be studied with some substituted anilines.

To verify whether the presence of dissolved oxygen causes aniline oxidation and thus biases isotope ratio measurements, we carried out SPME-GC/IRMS of samples that were prepared with anoxic stock and buffer solutions of the analytes at all relevant pH values in an anoxic glovebox (data not shown). Isotope signatures were identical regardless of the dissolved oxygen content of the solution and thus no effort to deoxygenate solutions was made in this study.

Detection Limits for Accurate Isotope Ratio Measurements. The operational detection limits for accurate stable isotope analysis of the investigated substituted anilines were derived from repeated ^{15}N- and ^{13}C-SPME-GC/IRMS measurements using PDMS/DVB fibers, aqueous solutions buffered with 10 mM MES at pH 7 (I = 4 M), and different analyte concentrations corresponding to peak amplitudes between 300 and 2500 mV and 500 and 6000 mV for N and C isotope analysis, respectively. As specified in the discussion below, detection limits correspond to the lowest analyte concentration lying within a $\Delta\delta^h$E-interval defined by the precision and accuracy of $\delta^{15}N$- and $\delta^{13}C$-measurements.

DFT-Calculations. The geometries of all free base anilines and their protonated conjugate acids were fully optimized at the density functional (DFT) level using the gradient-corrected Perdew−Wang exchange and correlation functionals[38,39] as modified by Adamo and Barone[40] in conjunction with the 6-311+G-(d) basis set.[41] Stationary equilibrium structures were confirmed by analytical calculation of vibrational frequencies, which were also used in the construction of ideal-gas, rigid-rotator, harmonic oscillator partition functions, from which thermal contributions to free energies G were computed.[42] Equilibrium isotope effects were computed as

$$EIE^N_{B-BH^+} = \frac{^{14}N K_B}{^{15}N K_B} = \exp\left(\frac{-G_{^{14}BH^+} + G_{^{14}B} + G_{^{15}BH^+} - G_{^{15}B}}{RT}\right) \quad (3)$$

dx.doi.org/10.1021/ac102667y |Anal. Chem. 2011, 83, 1641–1648

Table 2. Comparison of δ^{15}N- and δ^{13}C-Values of Substituted Anilines Measured by EA-IRMS and SPME-GC/IRMS[a]

compound	δ^{15}N (‰)		$\Delta\delta^{15}$N (‰)	δ^{13}C(‰)		$\Delta\delta^{13}$C (‰)
	EA-IRMS	SPME-GC/IRMS		EA-IRMS	SPME-GC/IRMS	
An	7.6 ± 0.3	7.9 ± 0.3	0.3 ± 0.5	−30.0 ± 0.3	−29.1 ± 0.2	0.9 ± 0.4
2-CH_3-An	3.7 ± 0.3	3.9 ± 0.3	0.2 ± 0.4	−27.5 ± 0.3	−27.8 ± 0.6	−0.3 ± 0.7
4-CH_3-An	−5.1 ± 0.3	−4.8 ± 0.2	0.3 ± 0.4	−28.3 ± 0.3	−27.8 ± 0.3	0.5 ± 0.5
2-Cl-An	6.4 ± 0.3	6.5 ± 0.6	0.1 ± 0.7	−26.7 ± 0.3	−26.7 ± 0.2	0.0 ± 0.3
4-Cl-An	−3.1 ± 0.3	−7.1 ± 0.9	−4.0 ± 0.9	−27.3 ± 0.3	−26.8 ± 0.5	0.5 ± 0.6

[a] SPME was performed in 10 mM MES buffered solutions at pH 7.0. The accuracy of the SPME-GC/IRMS-measurements is expressed as deviation from reference measurements of the pure analytes by EA-IRMS ($\Delta\delta^{h}$E-values). All uncertainties correspond to ±1 standard deviation (n = 3).

where $EIE^{N}_{B-BH^+}$ is the N equilibrium isotope effect and K_B is the equilibrium constant associated with aromatic amine protonation. The isotopically sensitive free energy G was determined for the substituted anilines, that is the neutral (G_{14_B},G_{15_B}) and protonated isotopologues ($G_{14_{BH+}}$,$G_{15_{BH+}}$). $EIE^{N}_{B-BH^+}$ was calculated for *para*- and *ortho*-substituted anilines including aromatic substituents with different electron donating and accepting properties (i.e., 4-N(CH_3)$_2$, 4-OCH_3, 4-CH_3, 4-F, 4-Cl, 4-NO_2 and 2-CH_3, 2-Cl). The corresponding $EIE^{C}_{B-BH^+}$ was calculated only for 4-CH_3-aniline and for each single carbon atom. All calculations made use of the Gaussian 03 electronic structure program suite.[43]

RESULTS AND DISCUSSION

^{15}N and ^{13}C Signatures determined by SPME-GC/IRMS. The N and C isotope signatures (δ^{15}N and δ^{13}C) of the substituted anilines measured by SPME-GC/IRMS at pH 7 correspond well with independent isotope signature measurements by elemental analyzer-IRMS (EA-IRMS). As shown in Table 2 accuracies were < ±0.3‰ for N and < ±0.5‰ for C isotope signatures, respectively, as revealed by the differences measured by the two methods ($\Delta\delta^{15}N_{SPME-EA}$ and $\Delta\delta^{13}C_{SPME-EA}$, eq 2). These deviations were within typical uncertainties (±0.5‰,[44]) reported for δ^{15}N and δ^{13}C-measurements (Table 2). Only $\Delta\delta^{15}$N-value of 4-Cl-aniline showed a significant offset by −4‰. All isotope ratio measurements were highly linear within the amplitude range typically used for isotope analysis, that is, 300−5500 mV (see Experimental Section for details and example for 4-CH_3-aniline in Figure 1).

Despite good linearity, δ^{15}N-measurements of substituted anilines deviated substantially from the correct values if the solution pH approached or was below the pK_a of the substituted aniline's conjugate acid. We observed a decrease of δ^{15}N corresponding to a depletion of isotopically heavy nitrogen (^{15}N) in the measured analyte with decreasing pH. The most substantial ^{15}N depletion was observed for 4-CH_3-aniline (−15‰), 4-Cl-aniline (−22‰), and aniline (−17‰) at approximately 2 pH units below the pK_a of the conjugate acid. In contrast, no C isotope fractionation was found as the pH-value of solutions decreased under the identical conditions and δ^{13}C-values remained constant within <0.9‰ (Figures 2 and 3). The observation of pH-dependent N isotope fractionation coincided with decreasing extraction efficiencies of the analytes from aqueous solution. Figure 1 illustrates the m/z 28 IRMS signal intensities of 4-CH_3-aniline between pH-values 4.0 and 7.0, which suggest that only neutral molecules are adsorbed to the SPME fiber while protonated species remain dissolved. The same

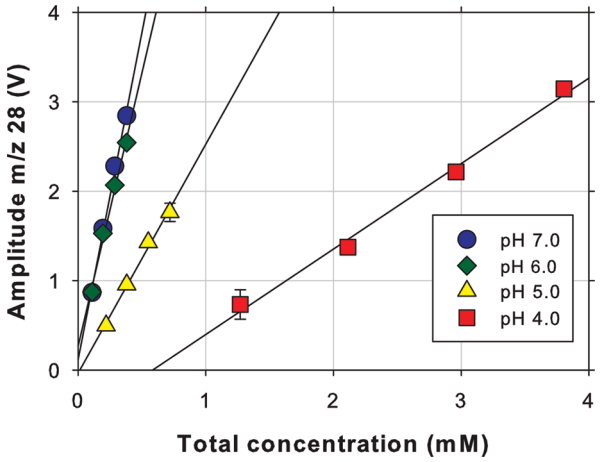

Figure 1. pH-dependence of 4-CH_3-aniline m/z 28 IRMS signal intensities for ^{15}N-SPME-GC/IRMS (fiber material PDMS/DVB) vs total aqueous 4-CH_3-aniline concentration in 10 mM MES (pH 6.0 and 7.0) and 10 mM acetate (pH 4.0 and 5.0) buffered solutions. Uncertainties of signal intensities are ± standard deviation (error bars mostly smaller than markers).

observation was made for other substituted anilines (data not shown). The decreasing δ^{15}N-values measured in adsorbed analytes at low pH (^{15}N depletion) imply that protonated compounds are enriched with ^{15}N, while the total analyte concentration in control solutions, which were not subject to SPME, remained unchanged. In contrast to earlier work,[14] our data suggest that accurate determination of δ^{15}N and δ^{13}C in substituted anilines measured by SPME-GC/IRMS is feasible if the pH of analyte solutions is controlled and maintained at least 2 pH-units above the pK_a of the conjugate acid.

Equilibrium Isotope Effect (EIE) associated with the protonation of substituted anilines. The observation of δ^{15}N-decrease at lower solution pH values in combination with the preferential extraction of neutral substituted aniline species and the fact that a change of ambient pH did not affect C isotope composition implies a nitrogen equilibrium isotope effect originating from the protonation at the amino functional group. To obtain evidence for the magnitude of equilibrium isotope fractionation owing to N-atom protonation, we measured the δ^{15}N of the substituted anilines in solutions buffered with different organic buffers at pH-values between 3.5 and 7.0 and compared the outcome with reference isotope signatures ($\delta^{15}N_{ref}$) obtained by EA-IRMS as follows. According

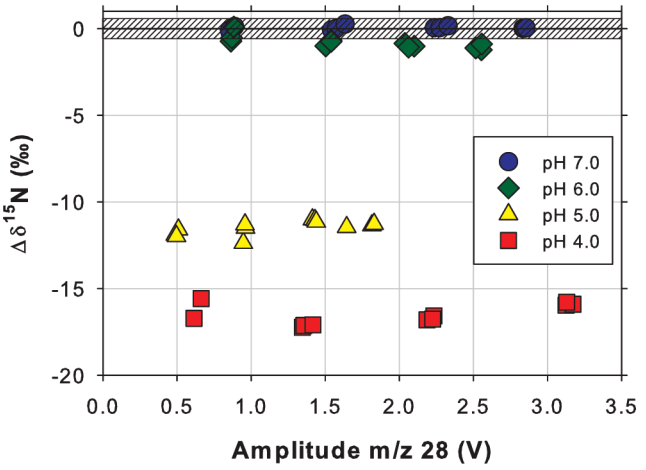

Figure 2. Accuracy of ^{15}N-SPME-GC/IRMS of 4-CH_3-aniline, $\Delta\delta^{15}N$, at solution pH-values between 4.0 and 7.0. Single $\delta^{15}N$ measurements at pH 6.0 and 7.0 were carried out in 10 mM MES buffer, those at pH 4.0 and 5.0 in 10 mM acetate buffer. The horizontal bar corresponds to the reference $\delta^{15}N$ (±standard deviation) of the pure 4-CH_3-aniline determined by EA-IRMS.

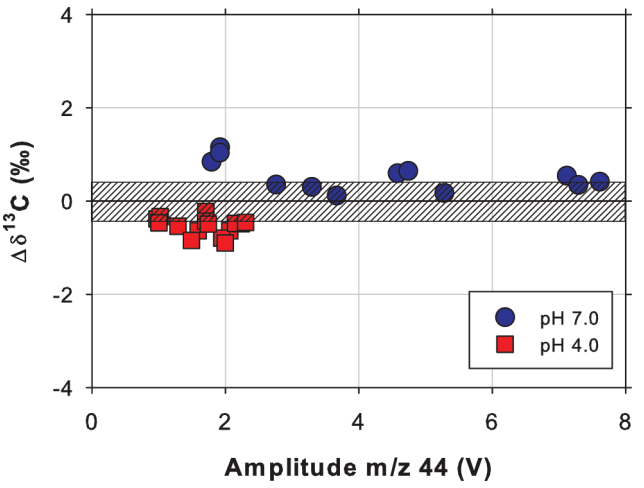

Figure 3. Accuracy of ^{13}C-SPME-GC/IRMS of 4-CH_3-aniline, $\Delta\delta^{13}C$, at solution pH-values 4.0 and 7.0. Single $\delta^{13}C$ measurements at pH 4.0 and 7.0 were carried out in 10 mM acetate and MES buffer, respectively. The horizontal bar corresponds to the reference $\delta^{13}C$ (±standard deviation) of the pure 4-CH_3-aniline determined by EA-IRMS.

to the isotopic mass balance $\delta^{15}N_{ref}$ corresponds to the sum of neutral and the protonated aniline species (eq 4).

$$\delta^{15}N_{ref} = f_{BH^+} \times \delta^{15}N_{BH^+} + (1 - f_{BH^+}) \times \delta^{15}N_B \quad (4)$$

where f_{BH^+} is the fraction of the protonated species, and $\delta^{15}N_{BH^+}$ and $\delta^{15}N_B$ are the N isotope signatures of protonated and neutral species, respectively. The partitioning of N isotopes between protonated and neutral compounds is described by the isotopic fractionation factor α_{B-BH^+} and corresponds to the ratio of isotopic composition in each species[45]

$$\alpha^N_{B-BH^+} = \frac{R_{BH^+}}{R_B} \quad (5)$$

where R_{BH^+} and R_B are the measured $^{15}N/^{14}N$ ratios in the protonated and neutral species, respectively, typically reported in the per mil notation as in eq 1. Substitution of a modified eq 1 into eq 5 results in an expression, which can be inserted into eq 4 to yield the measured, neutral isotope signature $\delta^{15}N_B$ at any solution pH as function of the degree of protonation, f_{BH^+}, the reference isotope signature, $\delta^{15}N_{ref}$, and the fractionation factor $\alpha^N_{B-BH^+}$ (eq 6).

$$\delta^{15}N_B = \frac{\delta^{15}N_{ref} - f_{BH^+} \times 1000 \times (\alpha^N_{B-BH^+} - 1)}{f_{BH^+} \times (\alpha^N_{B-BH^+} - 1) + 1} \quad (6)$$

For typical isotope effects, the term $f_{BH^+} \times (\alpha^N_{B-BH^+} - 1)$ becomes negligible and eq 6 simplifies to

$$\delta^{15}N_B \approx \delta^{15}N_{ref} - f_{BH^+} \times 1000 \times (\alpha^N_{B-BH^+} - 1) \quad (7)$$

Using N isotope enrichment factors instead of fractionation factors (eq 8), the extent of equilibrium isotope fractionation is the slope of the correlation of measured $\delta^{15}N$ (ascribed to neutral species) vs f_{BH^+} (eq 9).

$$\varepsilon^N_{B-BH^+} = 1000 \times (\alpha^N_{B-BH^+} - 1) \quad (8)$$

$$\delta^{15}N_B = \delta^{15}N_{ref} - f_{BH^+} \times \varepsilon^N_{B-BH^+}$$
$$= \delta^{15}N_{ref} + (1 - f_{BH^+}) \times \varepsilon^N_{B-BH^+} \quad (9)$$

Figure 4 shows the correlation of the measured $\delta^{15}N$ of aniline vs the fraction of neutral aniline species, $(1 - f_{BH^+})$, in solution buffered with different organic buffers over a wide pH range. Notice that $(1 - f_{BH^+})$ was calculated after pH measurements at high ionic strength owing to the addition of NaCl for extraction of the analytes. The slope of the regression line corresponds to an $\varepsilon^N_{B-BH^+}$-value of 18.8 ± 1.1‰ or an inverse equilibrium isotope effect, $EIE^N_{B-BH^+}$, of 0.9815 ± 0.0011 (eq 10, Table 4). The inverse $EIE^N_{B-BH^+}$ reflects the formation of an additional bond to N in the protonated species[46]

$$EIE^N_{B-BH^+} = \frac{^{14}N K_B}{^{15}N K_B} = \frac{1}{1 + \varepsilon^N_{B-BH^+}/1000}$$
$$= \frac{1}{(\alpha^N_{B-BH^+} - 1)} \quad (10)$$

Some of the $\delta^{15}N$ of aniline measured in solutions containing citrate and succinate buffer deviated by up to 3‰ from the expected values. These deviations presumably originate from high ionic strength effects, which result in altered activities and ionization constants of dissolved ions, buffers, and substituted anilines due to ion pairing with the electrolyte (NaCl).[47,48] While ion pairing models allow for estimates of activity coefficients and ionization constants of typical ions in saline waters,[49,50] no data are available for assessing the buffers and substituted anilines used in this work. Ionic strength effects might ultimately lead to different estimates of the fraction of neutral and protonated aniline concentrations and thus explain the lack of correlation for selected data points in Figure 4. As illustrated in Figure S1 (Supporting Information (SI)), however, this phenomenon does not alter the $\varepsilon^N_{B-BH^+}$-value obtained from eq 9 beyond experimental uncertainty.

The $EIE^N_{B-BH^+}$ obtained from Figure 4 is in excellent agreement with data inferred from the chromatographic separation of

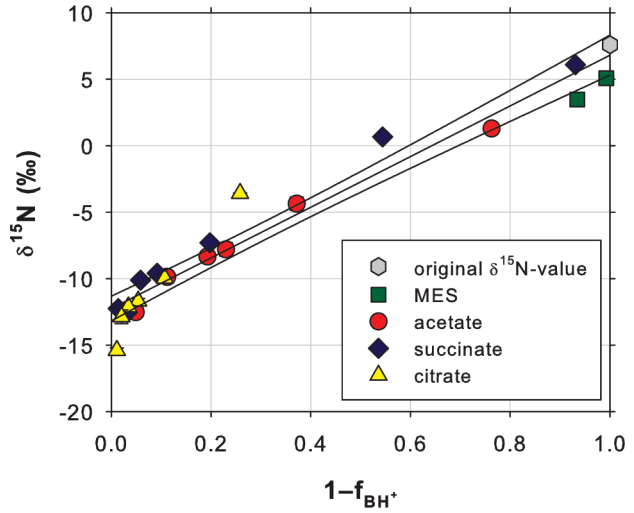

Figure 4. δ^{15}N-values of aniline determined by SPME-GC/IRMS vs the fraction of neutral aniline species in aqueous solution at different pH-values. Organic buffers used include: MES (pH-range 5.0−7.0), acetate (4.0−5.0), citrate (3.0−5.5), and succinate (3.5−6.5). The slope of the regression line corresponds to the enrichment factor $\varepsilon^{N}_{B-BH^+}$. Error bars of triplicate δ^{15}N measurements (±standard deviation) are smaller than the corresponding markers.

^{14}N and ^{15}N aniline isotopologues[51] and implies that the base dissociation constant of the ^{15}N-containing aniline species $^{15}K_B$, exceeds that of the light isotopologues, $^{14}K_B$. An $EIE^{N}_{B-BH^+}$ of 0.9815 in case of aniline (Table 3) implies that pK_B^{14N} exceeds pK_B^{15N} by 0.008 units. Thus, at any solution pH, the slightly higher basicity of the neutral ^{15}N-aniline causes the heavy (^{15}N) isotopologues to protonate to a larger extent compared to ^{14}N-aniline species because of stronger N−H bonds in the heavy isotope-containing conjugate acid. As only the deprotonated, that is, neutral compound is extracted by SPME, one therefore observes a depletion of ^{15}N and more negative δ^{15}N-values unless aromatic amine protonation is negligible at the solution pHs exceeding the pK_a of the conjugate acid by at least 2 units.

We investigated the effects of aromatic substituents on the variability of $EIE^{N}_{B-BH^+}$ with additional experiments for 4-CH_3-aniline and 4-Cl-aniline and through density functional theory (DFT) calculations for a wide set of compounds. The results are reported in Table 3 and in the SI. The ^{13}C-EIE value reported in Table 3 corresponds to the average calculated for all carbon atoms 1 to 7. This accounts for the fact that the heavy carbon atom is more or less evenly distributed over all molecular positions so that the value measured by CSIA represents the average of all position-specific isotope effects. The data compiled in Table 3 show excellent agreement between experiment and theory confirming inverse $EIE^{N}_{B-BH^+}$-values for all substituted anilines. In addition, $EIE^{N}_{B-BH^+}$-values show little sensitivity to aromatic substitution albeit a slight trend to more inverse isotope effects with increasing electron-donating properties of the substituent (and vice versa) is observed. Note that our calculations also confirm the absence of significant C isotope fractionation (4-CH_3-aniline $EIE^{C}_{B-BH^+}$ of 1.0011, Figure 3 and SI).

Detection Limits for Accurate Isotope Analysis of Substituted Anilines. Current recommendations[44,52−55] regarding detection limits for isotope ratio measurements by GC/IRMS not only include the precision of repeated measurements but also account for accuracy and the rather narrow linear range continuous-flow isotope ratio measurements. To this end, we determined the lowest analyte concentrations, at which the δ^{15}N- and δ^{13}C-values did not deviate from the reference isotope signatures determined by EA-IRMS by more than the accuracy of the proposed method (i.e., between 0.3‰ and 0.9‰ in $\Delta\delta^{15}$N and $\Delta\delta^{13}$C (SPME vs EA, Table 2)). The results summarized in Tables 2 and 4 for five substituted anilines illustrate that the use of buffered solutions and PDMS/DVB fibers for SPME not only improved accuracy but also allowed for more sensitive quantification of isotope ratios in the μg to mg L^{-1}-range, which represents an improvement by a factor of 2 compared to earlier approaches.[14]

Note that previous contributions, which focus predominantly on δ^{13}C measurements, refer to typical intervals of ±0.5‰ as acceptable uncertainties, from which the lowest acceptable concentration is deduced.[52,53] Unfortunately, these limits are not as established for less common isotope systems such as N and O isotope ratios. Uncertainties of δ^{15}N-values for organic compounds determined by GC/IRMS lack widely accepted limits across different isotope laboratories because these measurements are carried out less frequently than C isotope analyses. Given these ambiguities, we feel that it is more appropriate in the present case to define the acceptable limit of uncertainty for every compound individually because factors such as SPME extraction efficiency and the efficacy of combustion (and reduction) to analyte gases (N_2 and CO_2) cannot be assumed to be identical for all organic compounds analyzed for a specific isotope ratio.

Table 3. Nitrogen Isotope Enrichment Factors, $\varepsilon^{N}_{B-BH^+}$, and N Equilibrium Isotope Effects, $EIE^{N}_{B-BH^+}$, Associated with the Protonation of the Substituted Anilines: Comparison of Experimental (exp) and Theoretical Data (calc)

compound	experimental $\varepsilon^{N}_{B-BH^+}$ (‰)	$EIE^{N}_{B-BH^+}$, exp (−)	Theoretical $EIE^{N}_{B-BH^+}$, calc (−)
An	18.8 ± 1.1	0.9815 ± 0.0011	0.9811
2-CH_3-An	17.2 ± 1.8	0.9831 ± 0.0018	0.9811
4-CH_3-An	19.9 ± 4.1	0.9804 ± 0.0041	0.9811
2-Cl-An	17.2 ± 1.2	0.9831 ± 0.0012	0.9811
4-Cl-An	18.6 ± 2.0	0.9817 ± 0.0020	0.9821
4-N(CH_3)$_2$-An	-	-	0.9718
4-OCH_3-An	-	-	0.9800
4-F-An	-	-	0.9894
4-NO_2-An	-	-	0.9842

Table 4. Concentration Limits for Accurate N and C Isotope Analysis of Substituted Anilines by SPME-GC/IRMS Using PDMS/DVB Fibers

compound	δ^{15}N (mg L^{-1})	δ^{13}C (mg L^{-1})
An	1.4	0.37
2-CH_3-An	1.3	0.21
4-CH_3-An	2.1	0.54
2-Cl-An	1.9	<0.13
4-Cl-An	<0.64	0.26

CONCLUSION

Our study demonstrates the importance of adjusting the solution pH prior to compound-specific isotope ratio measurements

of substituted anilines by SPME-GC/IRMS. Because the conjugate acids of many substituted anilines exhibit pK_a-values between 2.5 and 7,[16,30] the fraction of protonated species will be significant given the range of pH-values of natural waters (pH 5−8,[56]). Besides compromising the sensitivity of the analytical method, δ^{15}N-measurements by SPME-GC/IRMS might deviate by up to −20‰ depending on the contaminant's basicity and the pH of the aqueous sample.

Moreover, the equilibrium N isotope fractionation associated with protonation of aryl N atoms could potentially interfere with the quantification of N isotope fractionation during contaminant transformation if the latter involves reactions at N-containing functional groups. Even though the magnitude of C and N isotope fractionation for (bio)degradation processes of substituted anilines are currently unknown, recent work with structurally related organic contaminants supports this conclusion. Protonations of alkyl-, aryl-, and triazine-bound N atoms are important elementary reaction steps during hydrolysis of phenylurea and triazine herbicides.[13,31,32,57] For the hydrolysis of isoproturon, an inverse N equilibrium isotope effect of 0.992 was reported for the alkyl-N protonation during initial zwitterion formation,[31] which contributed partly to the overall, observable N isotope fractionation. The N-heteroatom protonation in the triazine ring of atrazine associated with its acid-catalyzed and biotic hydrolysis led to apparent kinetic N isotope effects of similar inverse magnitude (0.974−0.995[32]). These inverse isotope effects were rationalized as a consequence of N atom hybridization changes or additional bonds to N in the transition state. Our interpretation of stronger N−H bonds in protonated heavy N isotopologues of substituted anilines due to inverse N equilibrium isotope effects in a similar range fully agrees with these findings.

■ ASSOCIATED CONTENT

Supporting Information. Position-specific ^{13}C-equilibrium isotope effects associated with 4-CH_3-aniline protonation. This material is available free of charge via the Internet at http://pubs.acs.org.

■ AUTHOR INFORMATION

Corresponding Author

*Phone: +41 44 823 50 76, e-mail: thomas.hofstetter@eawag.ch.

■ ACKNOWLEDGMENT

This work was supported by the Swiss National Science Foundation (grant no. 200020-116447/1). We thank Jakov Bolotin for experimental support as well as Martin Elsner and C. Annette Johnson for valuable comments.

■ REFERENCES

(1) Hofstetter, T. B.; Berg, M. *TrAC Trends Anal. Chem.* **2011**, doi:10.1016/j.trac.2010.10.012.

(2) Aeppli, C.; Hofstetter, T. B.; Amaral, H. I. F.; Kipfer, R.; Schwarzenbach, R. P.; Berg, M. *Environ. Sci. Technol.* **2010**, *44*, 3705–3711.

(3) Dempster, H. S.; Lollar, B. S.; Feenstra, S. *Environ. Sci. Technol.* **1997**, *31*, 3193–3197.

(4) Vieth, A.; Muller, J.; Strauch, G.; Kastner, M.; Gehre, M.; Meckenstock, R. U.; Richnow, H. H. *Isot. Environ. Health Stud.* **2003**, *39*, 113–124.

(5) Hunkeler, D.; Aravena, R.; Berry-Spark, K.; Cox, E. *Environ. Sci. Technol.* **2005**, *39*, 5975–5981.

(6) Zwank, L.; Berg, M.; Elsner, M.; Schmidt, T. C.; Schwarzenbach, R. P.; Haderlein, S. B. *Environ. Sci. Technol.* **2005**, *39*, 1018–1029.

(7) Kuder, T.; Wilson, J. T.; Kaiser, P.; Kolhatkar, R.; Philp, P.; Allen, J. *Environ. Sci. Technol.* **2005**, *39*, 213–220.

(8) Hunkeler, D.; Butler, B. J.; Aravena, R.; Barker, J. F. *Environ. Sci. Technol.* **2001**, *35*, 676–681.

(9) Fischer, A.; Gehre, M.; Breitfeld, J.; Richnow, H. H.; Vogt, C. *Rapid Commun. Mass Spectrom.* **2009**, *23*, 2439–2447.

(10) Vogt, C.; Cyrus, E.; Herklotz, I.; Schlosser, D.; Bahr, A.; Herrmann, S.; Richnow, H.-H.; Fischer, A. *Environ. Sci. Technol.* **2008**, *42*, 7793–7800.

(11) Tobler, N. B.; Hofstetter, T. B.; Schwarzenbach, R. P. *Environ. Sci. Technol.* **2007**, *41*, 7773–7780.

(12) Tobler, N. B.; Hofstetter, T. B.; Schwarzenbach, R. P. *Environ. Sci. Technol.* **2008**, *42*, 7786–7792.

(13) Meyer, A. H.; Penning, H.; Lowag, H.; Elsner, M. *Environ. Sci. Technol.* **2008**, *42*, 7757–7763.

(14) Berg, M.; Bolotin, J.; Hofstetter, T. B. *Anal. Chem.* **2007**, *79*, 2386–2393.

(15) Bernstein, A.; Ronen, Z.; Adar, E.; Nativ, R.; Lowag, H.; Stichler, W.; Meckenstock, R. U. *Environ. Sci. Technol.* **2008**, *42*, 7772–7777.

(16) Schwarzenbach, R. P.; Gschwend, P. M.; Imboden, D. M. *Environmental Organic Chemistry*, 2nd ed.; John Wiley & Sons: New York, 2003.

(17) Hofmann, D.; Gehre, M.; Jung, K. *Isot. Environ. Health Stud* **2003**, *39*, 233–244.

(18) Macko, S. A.; Uhle, M. E.; Engel, M. H.; Andrusevich, V. *Anal. Chem.* **1997**, *69*, 926–929.

(19) Styring, A. K.; Sealy, J. C.; Evershed, R. P. *Geochim. Cosmochim. Acta* **2010**, *74*, 241–251.

(20) Penning, H.; Elsner, M. *Anal. Chem.* **2007**, *79*, 8399–8405.

(21) Hartenbach, A. E.; Hofstetter, T. B.; Tentscher, P. R.; Canonica, S.; Berg, M.; Schwarzenbach, R. P. *Environ. Sci. Technol.* **2008**, *42*, 7751–7756.

(22) Hartenbach, A. E.; Hofstetter, T. B.; Aeschbacher, M.; Sander, M.; Kim, D.; Strathmann, T. J.; Arnold, W. A.; Cramer, C. J.; Schwarzenbach, R. P. *Environ. Sci. Technol.* **2008**, *42*, 8352–8359.

(23) Hofstetter, T. B.; Neumann, A.; Arnold, W. A.; Hartenbach, A. E.; Bolotin, J.; Cramer, C. J.; Schwarzenbach, R. P. *Environ. Sci. Technol.* **2008**, *42*, 1997–2003.

(24) Fishbein, L. *The Handbook of Environmental Chemistry—Anthropogenic Compounds*; Springer: Berlin, Germany, 1984.

(25) Zhang, H. C.; Huang, C. H. *Environ. Sci. Technol.* **2005**, *39*, 4474–4483.

(26) Laha, S.; Luthy, R. G. *Environ. Sci. Technol.* **1990**, *24*, 363–373.

(27) Simmons, K. E.; Minard, R. D.; Bollag, J. M. *Environ. Sci. Technol.* **1987**, *21*, 999–1003.

(28) Parris, G. E. *Environ. Sci. Technol.* **1980**, *14*, 1099–1106.

(29) Shin, K. A.; Spain, J. C. *Appl. Environ. Microbiol.* **2009**, *75*, 2694–2704.

(30) Lu, H.; Chen, X.; Zhan, C. G. *J. Phys. Chem. C* **2007**, *111*, 10599–10605.

(31) Penning, H.; Cramer, C. J.; Elsner, M. *Environ. Sci. Technol.* **2008**, *42*, 7764–7771.

(32) Meyer, A. H.; Penning, H.; Elsner, M. *Environ. Sci. Technol.* **2009**, *43*, 8079–8085.

(33) Zwank, L.; Berg, M.; Schmidt, T. C.; Haderlein, S. B. *Anal. Chem.* **2003**, *75*, 5575–5583.

(34) Brand, W. A.; Tegtmeyer, A. R.; Hilkert, A. *Org. Geochem.* **1994**, *21*, 585–594.

(35) Lehmann, M. F.; Bernasconi, S. M.; Barbieri, A.; McKenzie, J. A. *Geochim. Cosmochim. Acta* **2002**, *66*, 3573–3584.

(36) Merritt, D. A.; Hayes, J. M. *Anal. Chem.* **1994**, *66*, 2336–2347.

(37) Merritt, D. A.; Hayes, J. M. *J. Am. Soc. Mass Spectrom.* **1994**, *5*, 387–397.

(38) Perdew, J. P.; Yue, W. *Phys. Rev. B* **1986**, *33*, 8800–8802.

(39) Perdew, J. P. In *Electronic Structure of Solids '91*; Ziesche, P., Eschrig, H., Eds.; Akademie Verlag: Berlin, 1991, pp 11−20.
(40) Adamo, C.; Barone, V. *J. Chem. Phys.* **1998**, *108*, 664–675.
(41) Hehre, W. J.; Radom, L.; Schleyer, P. v. R.; Pople, J. A. *Ab Initio Molecular Orbital Theory*; Wiley: New York, 1986.
(42) Cramer, C. J. *Essentials of Computational Chemistry: Theories and Models*; 2nd ed.; John Wiley & Sons Ltd.: Chichester, 2004.
(43) Frisch, M. J.; Trucks, G. W.; Schlegel, H. B.; Scuseria, G. E.; Robb, M. A.; Cheeseman, J. R.; Montgomery, J. A., Jr.; Vreven, T.; Kudin, K. N.; Burant, J. C.; Millam, J. M.; Iyengar, S. S.; Tomasi, J.; Barone, V.; Mennucci, B.; Cossi, M.; Scalmani, G.; Rega, N.; Petersson, G. A.; Nakatsuji, H.; Hada, M.; Ehara, M.; Toyota, K.; Fukuda, R.; Hasegawa, J.; Ishida, M.; Nakajima, T.; Honda, Y.; Kitao, O.; Nakai, H.; Klene, M.; Li, X.; Knox, J. E.; Hratchian, H. P.; Cross, J. B.; Bakken, V.; Adamo, C.; Jaramillo, J.; Gomperts, R.; Stratmann, R. E.; Yazyev, O.; Austin, A. J.; Cammi, R.; Pomelli, C.; Ochterski, J. W.; Ayala, P. Y.; Morokuma, K.; Voth, G. A.; Salvador, P.; Dannenberg, J. J.; Zakrzewski, V. G.; Dapprich, S.; Daniels, A. D.; Strain, M. C.; Farkas, O.; Malick, D. K.; Rabuck, A. D.; Raghavachari, K.; Foresman, J. B.; Ortiz, J. V.; Cui, Q.; Baboul, A. G.; Clifford, S.; Cioslowski, J.; Stefanov, B. B.; Liu, G.; Liashenko, A.; Piskorz, P.; Komaromi, I.; Martin, R. L.; Fox, D. J.; Keith, T.; Al-Laham, M. A.; Peng, C. Y.; Nanayakkara, A.; Challacombe, M.; Gill, P. M. W.; Johnson, B.; Chen, W.; Wong, M. W.; Gonzalez, C.; Pople, J. A. *Gaussian 03*, revision C.02; Gaussian, Inc.: Wallingford, CT, 2004.
(44) *A Guide for Assessing Biodegradation and Source Identification of Organic Ground Water Contaminants Using Compound Specific Isotope Analysis (CSIA)*; Hunkeler, D., Meckenstock, R. U., Sherwood Lollar, B., Schmidt, T. C.,Wilson, J. T., Eds.; U.S. EPA: Washington, DC, 2008.
(45) Wolfsberg, M.; Van Hook, W. A.; Paneth, P.; Rebelo, L. P. N. *Isotope Effects in the Chemical, Geological, and Bio Sciences*; Springer: New York, 2010.
(46) Marlier, J. F. *Acc. Chem. Res.* **2001**, *34*, 283–290.
(47) Millero, F. J. *Geochim. Cosmochim. Acta* **1981**, *45*, 2085–2089.
(48) Pitzer, K. S. *J. Phys. Chem.* **1973**, *77*, 268–277.
(49) Pitzer, K. S. In *Activity Coefficients in Electrolyte Solutions*,; Pytkovitz, R. M., Ed.; CRC Press: Boca Raton, 1991; Vol. 2, pp 75−153.
(50) Millero, F. J.; Schreiber, D. R. *Am. J. Sci.* **1982**, *282*, 1508–1540.
(51) Tanaka, N.; Yamaguchi, A.; Araki, M.; Kimata, K. *J. Am. Chem. Soc.* **1985**, *107*, 7781–7782.
(52) Jochmann, M. A.; Blessing, M.; Haderlein, S. B.; Schmidt, T. C. *Rapid Commun. Mass Spectrom.* **2006**, *20*, 3639–3648.
(53) Lollar, B. S.; Hirschorn, S. K.; Chartrand, M. M. G.; Lacrampe-Couloume, G. *Anal. Chem.* **2007**, *79*, 3469–3475.
(54) Hunkeler, D.; Bernasconi, S. M. In *Environmental Isotopes in Biodegradation and Bioremediation*, ed.; Aelion, M. C., Höhener, P., Hunkeler, D., Aravena, R., Eds.; CRC Press: Boca Raton, 2010; pp 23−42.
(55) Blessing, M.; Jochmann, M. A.; Schmidt, T. C. *Anal. Bioanal. Chem.* **2008**, *390*, 591–603.
(56) Stumm, W.; Morgan, J. J. *Aquatic Chemistry*, 3rd ed.; John Wiley & Sons: New York, 1996.
(57) Dybala-Defratyka, A.; Szatkowski, L.; Kaminski, R.; Wujec, M.; Siwek, A.; Paneth, P. *Environ. Sci. Technol.* **2008**, *42*, 7744–7750.
(58) Colon, D.; Weber, E. J.; Baughman, G. L. *Environ. Sci. Technol.* **2002**, *36*, 2443–2450.